

# Growth of matter perturbations in clustered holographic dark energy cosmologies

Ahmad Mehrabi,<sup>1,\*</sup> Spyros. Basilakos,<sup>2,†</sup> Mohammad Malekjani,<sup>1,‡</sup> and Zahra Davari<sup>1</sup>

<sup>1</sup>*Department of Physics, Bu-Ali Sina University, Hamedan 65178, 016016, Iran*

<sup>2</sup>*Academy of Athens, Research Center for Astronomy & Applied Mathematics, Soranou Efessiou 4, 11-527, Athens, Greece* <sup>†</sup>

We investigate the growth of matter fluctuations in holographic dark energy cosmologies. First we use an overall statistical analysis involving the latest observational data in order to place constraints on the cosmological parameters. Then we test the range of validity of the holographic dark energy models at the perturbation level and its variants from the concordance  $\Lambda$  cosmology. Specifically, we provide a new analytical approach in order to derive, for the first time, the growth index of matter perturbations. Considering a homogeneous holographic dark energy we find that the growth index is  $\gamma \approx \frac{4}{7}$  which is somewhat larger ( $\sim 4.8\%$ ) than that of the usual  $\Lambda$  cosmology,  $\gamma^{(\Lambda)} \approx \frac{6}{11}$ . Finally, if we allow clustering in the holographic dark energy models then the asymptotic value of the growth index is given in terms of the effective sound speed  $c_{\text{eff}}^2$ , namely  $\gamma \approx \frac{3(1-c_{\text{eff}}^2)}{7}$ .

PACS numbers: 98.80.-k, 95.36.+x

## I. INTRODUCTION

The current accelerated expansion of the Universe [1–4] can be well explained either by introducing the so called dark energy (hereafter DE), namely an exotic cosmic fluid with a negative pressure, or by modifying the standard theory of gravity on extragalactic scales. Based on the Planck results [5] it has been found that that DE amounts to  $\sim 69\%$  while the matter component (cold dark matter+baryons) corresponds to  $\sim 31\%$  of the current total energy budget, respectively.

In this framework, a large family of cosmological models have been proposed in order to explain the origin of the cosmic acceleration (for a comprehensive review see [6]). The simplest DE candidate is the well known cosmological constant for which the equation of state (hereafter EoS) parameter is strictly equal to -1 and thus the DE is connected with the energy of vacuum. Although the concordance  $\Lambda$  cosmology is consistent with the available observational data it has two weak points: the fine-tuning and the cosmic coincidence [6–11]. Alternatively, in the last two decades, a wealth of dynamical DE models with a time-varying EoS have been studied in the literature [6, 12, 13] in order to circumvent the above cosmological puzzles. However, the majority of DE models are based on purely phenomenological arguments.

In this work we focus on the holographic dark energy (HDE) scenario which has a strong theoretical motivation. Indeed the HDE model originates from the fundamental holographic principle in quantum gravity theory [14]. In particular, according to the holographic principle, the number of degrees of freedom for a finite-size system is finite and bounded by the area of its boundary [15]. Therefore, applying the holographic principle in

cosmology, namely considering the future event horizon for IR cut-off one can show that the energy density of DE is given by (see Refs. [16–22])

$$\rho_d = 3s^2 M_{Pl}^2 R_h^{-2}, \quad (1)$$

where  $s$  is a constant,  $M_{Pl}^2 = 1/8\pi G$  is the reduced Plank mass and the coefficient 3 is just for convenience. Notice, that the event horizon is written as

$$R_h = a \int_t^\infty \frac{dt}{a(t)} = a \int_a^\infty \frac{da}{a^2 H(a)}, \quad (2)$$

where  $a(t)$  is the scale factor of the universe,  $H(a) = \frac{\dot{a}}{a}$  is the Hubble parameter and  $t$  is the cosmic time. Interestingly, it has been found that the HDE cosmological pattern provides the current cosmic acceleration and it is in agreement with the observational data [23–37]. Moreover, in this scenario the coincidence as well as the fine-tuning problems are successfully alleviated [22].

However, in addition to the background evolution, the formation of large scale structures provides valuable information about the nature of DE [38]. Indeed, matter perturbations can grow via the gravitational instability during the different epochs of the cosmic history. In fact, DE component not only accelerates the expansion of the Universe but also it affects the growth rate of matter perturbations [39]. It becomes clear that the latter opens a new avenue towards understanding the mechanism of structure formation in the DE regime.

From the observational viewpoint, it is worthwhile to set up a more general formalism in which the background data (SnIa, BAOs, CMB shift parameter etc) are jointed to the growth data (Ref.[40] and references therein) in order to place constraints on the DE models. Concerning the HDE models such a joint analysis has given  $s = 0.750_{-0.0999}^{+0.0976}$  and  $\sigma_8 = 0.763_{-0.0465}^{+0.0477}$  [41], where  $\sigma_8$  is the variance of matter perturbations within the sphere of  $R = 8h^{-1}\text{Mpc}$  at present time. It is worth mentioning that the author of [41] has treated the holographic DE as homogeneous.

\* Mehrabi@basu.ac.ir

† svasil@academyofathens.gr

‡ malekjani@basu.ac.ir

Generally speaking, in the case of dynamical DE models, one can consider fluctuations in both time and space in a similar fashion to matter [42–45]. Potentially, since the energy density of HDE is defined according to event horizon IR cut-off, one may consider that the origin of the HDE perturbations is due to the fluctuations of the future event horizon [46]. In this case, it has been shown that the HDE adiabatic sound speed is positive and therefore the corresponding perturbations are stable (see [46]). As a matter of fact, the key parameter in order to describe the clustering of DE is the so called effective sound speed  $c_{\text{eff}}^2 = \delta p_d / \delta \rho_d$ . Usually, in the literature one can find the following two cases: (i) homogeneous DE with  $c_{\text{eff}}^2 = 1$  (in units of the speed of light) and (ii) inhomogeneous DE with  $c_{\text{eff}}^2 = 0$ . In the former case the sound horizon is equal or larger than the Hubble horizon which means that DE perturbations are taking place only at very large scales. On the other hand, in case (ii), the sound horizon is much smaller than the Hubble radius and thus DE perturbations can grow within the framework of gravitational instability in a similar manner to matter perturbations [47–50]. The scenario of DE clustering has been widely investigated in the literature [44, 51–61]. Although it is difficult to directly measure the amount of DE clustering, there are some indications that the homogeneous DE has some problems towards reproducing the observed concentration parameter of the massive galaxy clusters [62]. In the context of the spherical collapse model, it has been shown that inhomogeneous DE models fit better the growth data than the homogeneous DE scenarios [45, 63, 64].

Following the above lines, in this work we provide a comprehensive investigation of the HDE cosmological model at the background and perturbation levels respectively. The paper is organized as follows: in section (II) we first present the main ingredients of the HDE cosmologies. Then we study the growth matter perturbations in clustered HDE models and we discuss the variants from the homogeneous case. In section (III), we implement a joint likelihood analysis involving the latest cosmological data including those of growth in order to put constraints on the corresponding cosmological parameters. The growth index of the HDE models is determined for the first time in section IV. Finally we summarize our results in section (V).

## II. GROWTH OF PERTURBATIONS IN HDE COSMOLOGIES

Initially, we provide a brief discussion of the HDE cosmological model in the framework of Friedmann-Robertson-Walker (FRW) metric and then we derive the basic differential equations which guide the evolution of matter (with  $P_m = 0$ ) and DE perturbations. Phenomenologically, HDE can be treated as an effective dark energy fluid which means that one can use the continuity equation [see Eq.(6) with  $P_d = w_d \rho_d$ ]. Such a description

is widely used in this kind of studies (see for example [65] and references therein).

### A. HDE model

In the context of the flat FRW metric, the dynamics of the Universe containing pressure-less matter, radiation and DE fluids is given by

$$H^2 = \frac{8\pi G}{3}(\rho_m + \rho_r + \rho_d), \quad (3)$$

where  $H$  is the Hubble parameter,  $\rho_m$ ,  $\rho_r$  and  $\rho_d$  are the matter, radiation [66] and DE energy densities, respectively. Considering that interactions do not take place among the cosmic fluid components one may write the following continuity equations

$$\dot{\rho}_m + 3H\rho_m = 0, \quad (4)$$

$$\dot{\rho}_r + 4H\rho_r = 0, \quad (5)$$

$$\dot{\rho}_d + 3H(1 + w_d)\rho_d = 0, \quad (6)$$

where the dot is the derivative with respect to cosmic time and  $w_d$  is the DE equation of state (hereafter EoS) parameter. Differentiating Eq.(3) and using at the same time Eq. (1), the continuity equations (4, 5, 6) and the expression  $\dot{R}_h = 1 + HR_h$ , we can obtain the EoS parameter  $w_d$  of the HDE model

$$w_d(z) = -\frac{1}{3} - \frac{2\sqrt{\Omega_d(z)}}{3s}, \quad (7)$$

where  $\Omega_d(z) = 1 - \Omega_m(z)$  is the dimensionless energy density of the DE fluid and  $z$  is the redshift. At late enough times, due to the fact that DE dominates the cosmic expansion of the universe, we have  $\Omega_d \rightarrow 1$  which means that  $w_d \rightarrow -\frac{1}{3} - \frac{2}{3s}$ . Within this framework, if we suppose that  $w_d(z_*) = -1$  at the special epoch of  $z = z_*$  then the value  $s$  satisfies  $s = \sqrt{\Omega_d(z_*)}$ . At the present epoch,  $z_* = 0$ , and for  $\Omega_{d0} = \Omega_d(0) = 0.70$  we compute  $s \simeq 0.83$ . On the other hand, at large redshifts  $z \gg 1$  ( $\Omega_d \rightarrow 0$ ) it is easy to check that the asymptotic value of the EoS parameter is  $w_\infty \rightarrow -1/3$ .

Now, taking the time derivative of  $\Omega_d = \rho_d/\rho_s = 1/(HR_h)^2$ , we can obtain the evolution of  $\Omega_d$  in HDE models as follows

$$a\Omega'_d = -\frac{w_d}{3}\Omega_d(1 - \Omega_d), \quad (8)$$

where the prime is the derivative with respect to scale factor  $a$ . In terms of cosmic redshift  $z = 1/a - 1$ , Eq.(8) can be written as

$$\frac{d\Omega_d}{dz} = \frac{w_d(z)\Omega_d(z)}{3(1+z)} \left[ 1 - \Omega_d(z) \right]. \quad (9)$$

Using the Friedmann equation (3) and the continuity equations (4, 5), we can easily derive the evolution of

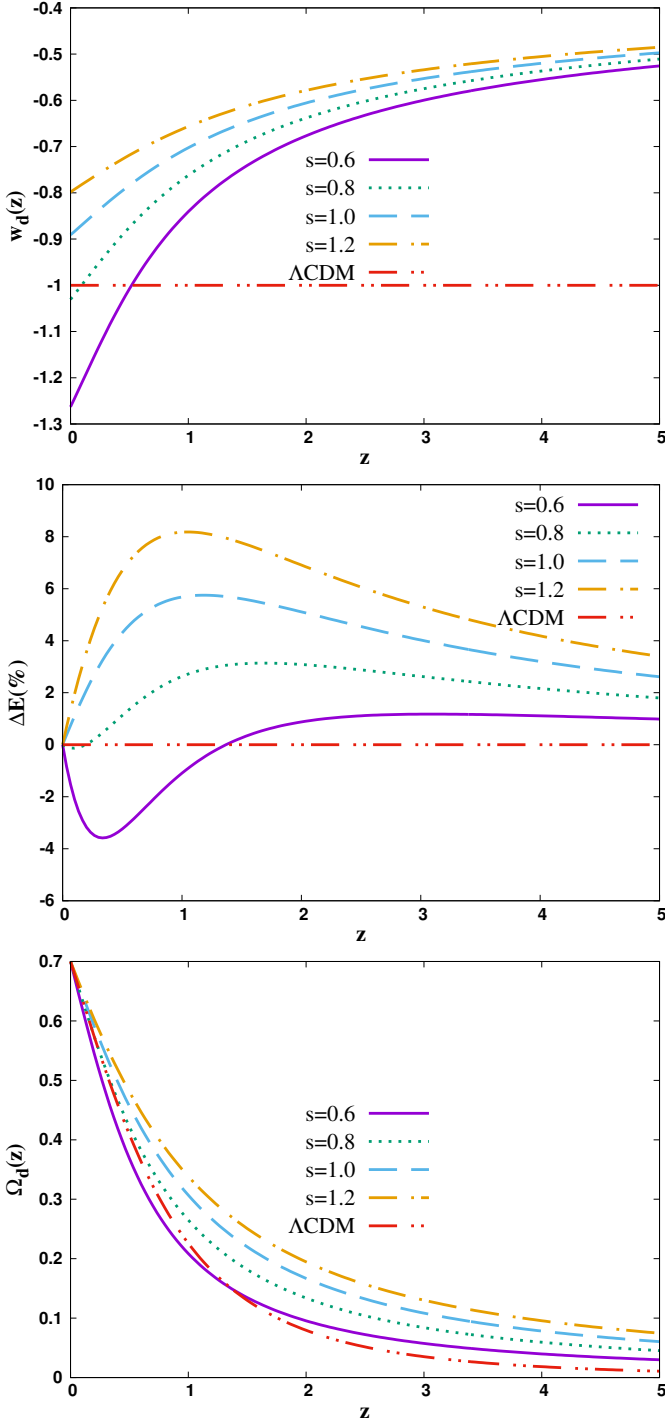


FIG. 1. *Top panel:* Evolution of the equation of state parameter of HDE model  $w_d$  as a function of cosmic redshift  $z$  for different values of the parameter  $s$ . *Middle panel:* The relative deviation  $\Delta E(z)$  of the normalized Hubble parameter for the HDE models with respect to  $\Lambda$ CDM. *Bottom panel:* The evolution of the DE density parameter  $\Omega_d$ . The dotted-dashed, dashed, dotted and solid curves correspond to HDE models with  $s = 1.2$ ,  $s = 1$ ,  $s = 0.8$  and  $s = 0.6$  respectively. Notice, that the reference  $\Lambda$ CDM model is shown by dashed-double-dotted line. In all cases we use  $\Omega_{d0} = 1 - \Omega_{m0} = 0.7$ .

the dimensionless Hubble parameter,  $E(z) = H(z)/H_0$  (where  $H_0$  is the Hubble constant), as follows:

$$E^2(z) = \frac{\Omega_{m0}(1+z)^3 + \Omega_{r0}(1+z)^4}{1 - \Omega_d(z)}. \quad (10)$$

Obviously, equations (7), (9) and (10) form a system whose solution provides the evolution of the main cosmological functions, namely  $E(z)$ ,  $w_d(z)$  and  $\Omega_d(z)$ . As an example, in the upper panel of Fig. (1), we present the evolution of the EoS parameter  $w_d(z)$  for the following HDE models  $s = 0.6$  (dashed line),  $s = 0.8$  (dotted line),  $s = 1$  (solid line) and  $s = 1.2$  (dot-dashed line). Notice, that all models are fixed to  $\Omega_{d0} = 0.7$  at the present time. As expected, for  $s = 0.8$  we reach the phantom regime prior to the present time. In the case of  $s = 0.6$  the EoS parameter crosses the phantom line  $w_d = -1$  at the epoch of  $z \sim 0.5$ , while for  $s = 1$  and  $s = 1.2$  it remains in quintessence regime for each  $z$ .

Since the Hubble expansion affects the growth of matter perturbations it is important to understand the behavior of the Hubble parameter in HDE cosmologies. In this context, we can appreciate in the middle panel of Fig. (1) the relative difference  $\Delta E(z)$  of the normalized Hubble parameters  $E_{\text{HDE}}(a)$  with respect to the  $\Lambda$ CDM solution  $E_{\Lambda\text{CDM}}(z)$

$$\Delta E(z) = 100 \times \left[ \frac{E(z)_{\text{HDE}}}{E(z)_{\Lambda\text{CDM}}} - 1 \right]. \quad (11)$$

For the quintessence HDE models ( $s = 1$  and  $s = 1.2$ ), we observe that the quantity  $\Delta E(z)$  is positive for all redshifts which means that the corresponding cosmic expansion is larger than that of the concordance  $\Lambda$ CDM model. There is a visible deviation from the latter around the epoch  $z \sim 0.7$ . This deviation becomes at the level of  $\sim +5\%$  and  $\sim +8\%$  for  $s = 1$  and  $s = 1.2$  respectively. On the other hand, in the case of phantom HDE models ( $w_d < -1$ ) we have a mixed situation. Specifically, using  $s = 0.6$  we can see that at  $z \sim 0.7$  the relative difference becomes at the level of  $\sim -3.5\%$ , while at high enough redshifts  $z \gg 1$  we find that  $E_{\text{HDE}}(z)$  deviates from  $E_{\Lambda\text{CDM}}(z)$  only by  $\sim +1\%$ . For  $s = 0.8$  the maximum relative difference is  $\sim +2.5\%$  at  $z \sim 1$ , while prior to the present epoch since  $w_{d0} \sim -1$  we have  $E_{\text{HDE}}(z=0) \rightarrow E_{\Lambda\text{CDM}}(z=0)$ .

Lastly, in the bottom panel of Fig. (1) we plot  $\Omega_d$  as a function of redshift. For the majority of the HDE models we find  $\Omega_d(z) > \Omega_\Lambda(z)$ . In the case of  $s = 0.6$  the amount of DE is a bit higher (lower) than that of  $\Lambda$ CDM model at high (low) redshifts.

## B. growth of perturbations in HDE models

Here we briefly discuss the main properties of the linear perturbation theory within the framework of HDE cosmologies. Following the general approach of [43] the

basic equations that describe the evolution of matter and DE perturbations are given by

$$\dot{\delta}_m + \frac{\theta_m}{a} = 0, \quad (12)$$

$$\dot{\delta}_d + (1 + w_d) \frac{\theta_d}{a} + 3H(c_{\text{eff}}^2 - w_d)\delta_d = 0, \quad (13)$$

$$\dot{\theta}_m + H\theta_m - \frac{k^2\phi}{a} = 0, \quad (14)$$

$$\dot{\theta}_d + H\theta_d - \frac{k^2 c_{\text{eff}}^2 \delta_d}{(1 + w_d)a} - \frac{k^2 \phi}{a} = 0. \quad (15)$$

where  $c_{\text{eff}}^2$  is the effective sound speed. It is well known that at sub-horizon scales one can extract the scale  $k$  from the above equations by utilizing the Poisson equation (see [40] and references therein)

$$-\frac{k^2}{a^2}\phi = \frac{3}{2}H^2[\Omega_m\delta_m + (1 + 3c_{\text{eff}}^2)\Omega_d\delta_d], \quad (16)$$

The amount of DE clustering depends on the magnitude of its effective sound speed  $c_{\text{eff}}^2$  and for  $c_{\text{eff}}^2 = 0$  DE clusters in a similar manner to dark matter. However, due to the presence of the DE pressure one may expect that the amplitude of the DE perturbations is relatively low with respect to that of dark matter. Notice, that below we set  $c_{\text{eff}}^2 = 0$ . In the current work we treat DE as a perfect fluid [67] which implies that the effective sound speed coincides with the adiabatic sound speed

$$c_a^2 = w_d - \frac{aw'_d}{3(1 + w_d)}. \quad (17)$$

where prime denotes derivative with respect to the scale factor,  $w'_d = dw_d/da$ .

Now eliminating  $\theta$  from the system of equations (12, 13, 14 and 15) and using  $\frac{d}{dt} = aH\frac{d}{da}$  we obtain after some calculations the following second order differential equations which describe the evolution of matter and DE perturbations respectively:

$$\delta_m'' + A_m\delta_m' + B_m\delta_m = \frac{3}{2a^2}(\Omega_m\delta_m + \Omega_d\delta_d), \quad (18)$$

$$\delta_d'' + A_d\delta_d' + B_d\delta_d = \frac{3}{2a^2}(1 + w_d)(\Omega_m\delta_m + \Omega_d\delta_d) \quad (19)$$

where the coefficients are

$$A_m = \frac{3}{2a}(1 - \Omega_d w_d), \quad (20)$$

$$B_m = 0,$$

$$A_d = \frac{1}{a} \left[ -3w_d - \frac{aw'_d}{1 + w_d} + \frac{3}{2}(1 - \Omega_d w_d) \right],$$

$$B_d = \frac{1}{a^2} \left[ -aw'_d + \frac{aw'_d w_d}{1 + w_d} - \frac{1}{2}w_d(1 - 3\Omega_d w_d) \right],$$

We would like to stress that Eqs.(18) and (19) are both valid in post-Newtonian and General Relativity (GR) formalisms respectively [40]. In order to measure the evolution of DE and matter fluctuations we numerically integrate the aforementioned equations from  $a = 0.001$  till

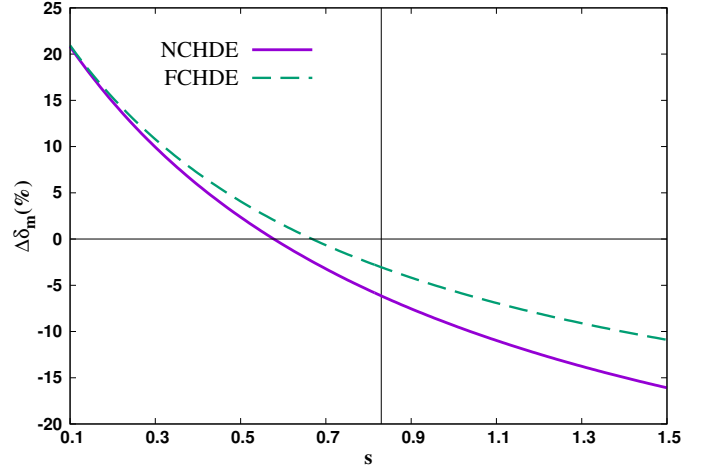


FIG. 2. The relative difference  $\Delta\delta_m(\%)$  at the present epoch versus  $s$ . The solid (dashed) lines stands for NCHDE (FCHDE) model. The vertical line indicates the  $w_d = -1$  ( $s = 0.83$  for  $\Omega_{d0} = 0.7$ ) line.

the present time  $a = 1$  ( $z = 0$ ). Regarding the initial conditions the situations is as follows. We use the conditions of [44]:

$$\delta'_{mi} = \frac{\delta_{mi}}{a_i}, \quad (21)$$

$$\delta_{di} = \frac{1 + w_d}{1 - 3w_d}\delta_{mi}, \quad (22)$$

$$\delta'_{di} = \frac{4w'_d}{(1 - 3w_d)^2}\delta_{mi} + \frac{1 + w_d}{1 - 3w_d}\delta'_{mi}, \quad (23)$$

where we set  $\delta_{mi} = 1.5 \times 10^{-4}$  which guarantees that matter perturbations are in the linear regime ( $\delta_{m0} \ll 1$ ). Here we focus on the following scenarios: (i) the holographic DE remains homogeneous ( $\delta_d = 0$ ) and only the corresponding matter component clusters (non-clustering holographic dark energy hereafter NCHDE) and (ii) clustered HDE assuming that the whole system fully clusters (matter and HDE), namely  $c_{\text{eff}}^2 = 0$  (full clustering holographic dark energy: FCHDE).

In figure (2) we show the relative deviation of the HDE matter fluctuations (at the current epoch) with respect to those of  $\Lambda$ CDM as a function of  $s$

$$\Delta\delta_m = 100 \times \left[ \frac{(\delta_{m0})_{\text{HDE}}}{(\delta_{m0})_{\Lambda\text{CDM}}} - 1 \right]. \quad (24)$$

Notice, that the vertical line at  $s = 0.83$  separates the phantom from the quintessence region [see discussion after Eq.(7)].

First we observe that  $\Delta\delta_m$  is a decreasing function of  $s$  and it lies in the interval  $(-20\%, 20\%)$ . These differences imply that the deviations of the HDE matter fluctuations depend on the initial assumptions and limitations imposed in the general system of equations (12), (13) and (21)-(23). Second we verify that for small values of  $s$  the Hubble friction ( $H\delta_m$ ) is small with respect to

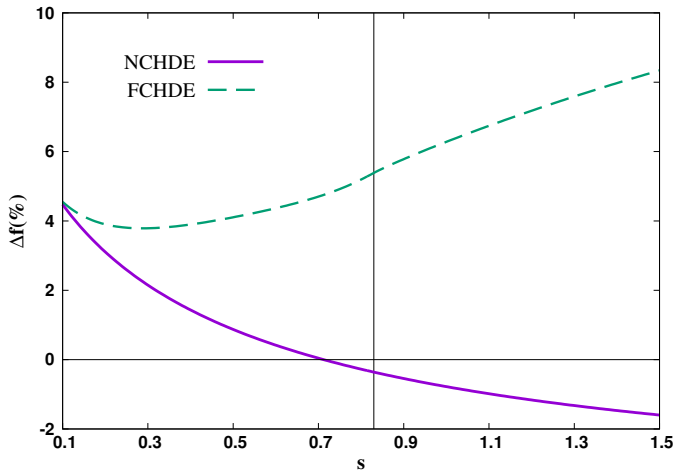


FIG. 3. The relative difference of the growth rate of clustering at present time as a function of  $s$ . The style of lines can be found in figure (2). The vertical line represents the phantom border, namely  $s = 0.83$  for  $\Omega_{d0} = 0.7$ .

that of  $\Lambda$ CDM (see also figure 1), which means that the corresponding matter fluctuations in NCHDE/FCHDE models are larger than those of the concordance  $\Lambda$  cosmology. The opposite is true for large values of  $s$ . Also, we find that the relative deviations between NCHDE and FCHDE models are negligible when  $s < 0.3$ . For  $s > 0.3$  the term  $\Omega_d \delta_d$  in Eq. (12) starts to get power and thus we have  $\delta_m^{(\text{FCHDE})} > \delta_m^{(\text{NCHDE})}$ .

Moreover, we calculate the growth rate of clustering in HDE models and compare it with concordance  $\Lambda$ CDM model. The growth rate function is given by  $f(a) = d \ln \delta_m / d \ln a$  [see Eq.(26) below]. In this case the corresponding relative difference is given by

$$\Delta f = 100 \times \left( \frac{f_{\text{HDE}}}{f_{\Lambda\text{CDM}}} - 1 \right). \quad (25)$$

In figure (3) we plot the quantity  $\Delta f(\%)$  at the present epoch as a function of  $s$ . Obviously, for the FCHDE model the growth rate of matter perturbations is always larger than  $\Lambda$ CDM. As an example, prior to the phantom line ( $s \sim 0.83$ ) we find a  $\sim 4\%$  difference. In the case of NCHDE model we see that  $\Delta f(\%)$  becomes positive (or negative) for  $s < 0.75$  (or  $s > 0.75$ ) and the relative difference is  $\sim 0.4\%$  at  $s \sim 0.83$ .

Finally, in figure (4) we plot  $\delta_{d0}$  versus  $s$  and we observe that the current DE perturbations increase, due to the term  $1 + w_d$  in equation (19), as a function of  $s$ . To this end, close to  $s \simeq 0.83$  we find that  $\delta_{d0} \simeq 0.008$ .

### III. HOLOGRAPHIC MODELS VERSUS DATA

In this section we attempt to compare the HDE models against the latest observational data. Specifically, we perform an overall statistical analysis using the geometri-

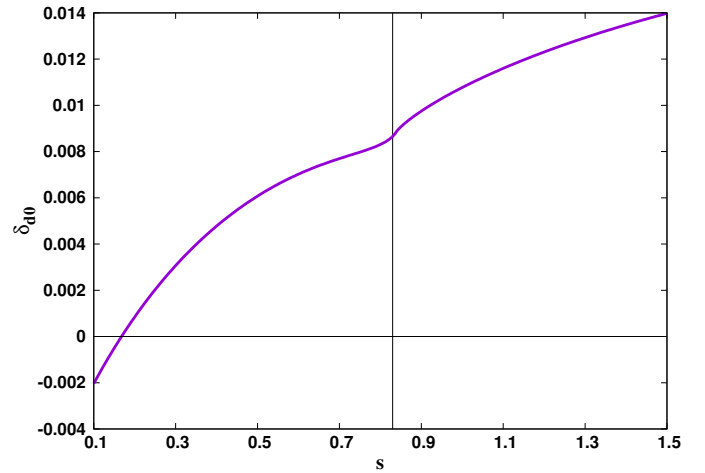


FIG. 4. DE perturbations at present time as a function of  $s$ . The vertical line presents the phantom border.

Parameters	HDE	$\Lambda$ CDM
$\Omega_{m0}$	$0.267^{+0.0019+0.0026}_{-0.0016-0.0028}$	$0.276^{+0.0017+0.0029}_{-0.0015-0.0027}$
$h$	$0.696^{+0.005+0.007}_{-0.004-0.007}$	$0.70^{+0.004+0.008}_{-0.005-0.009}$
$s$	$0.782^{+0.035+0.079}_{-0.033-0.075}$	—
$w_{d0}$	-1.062	-1.

TABLE I. The best fit values of parameters using the geometry measurements data set for HDE and concordance  $\Lambda$ CDM models.  $w_{d0}$  indicate the EoS at present time.

cal data (SnIa [68], BAO [69–72], CMB [73], Big Bang Nucleosynthesis [74, 75],  $H(z)$  data [76–79]) and the growth data as gathered by [40].

We would like to point that the geometrical data, the growth data, the covariances, the joint  $\chi^2_{\text{tot}}(\mathbf{p})$  function including that of the Akaike information criterion[80] and the MCMC algorithm are presented in [40]. The above statistical vector contains the corresponding cosmological parameters, namely  $\mathbf{p} = \{\Omega_{\text{DM}}, \Omega_{\text{b}}, h, s, \sigma_8\}$ , where  $\Omega_{\text{DM}}$  and  $\Omega_{\text{b}}$  are the dimensionless energy densities of pressure-less dark matter and baryons, respectively and  $\sigma_8$  is the variance of matter perturbations within the sphere of  $R = 8h^{-1}\text{Mpc}$  at present time. We would like to mention that the total  $\Omega_m(a)$  is written as  $\Omega_m(a) \equiv \Omega_{\text{DM}}(a) + \Omega_{\text{b}}(a)$ .

The observational constraints are summarized in Table I and II, where for the former case we utilize only the geometrical data while for the latter case we have included the growth data in the overall likelihood analysis. Specifically, we find the following.

In the case of the geometrical data,

- for the HDE model:  $\chi^2_{\text{min}} = 588.1$ ,  $n_{\text{fit}} = 4$  and AIC=596.1;



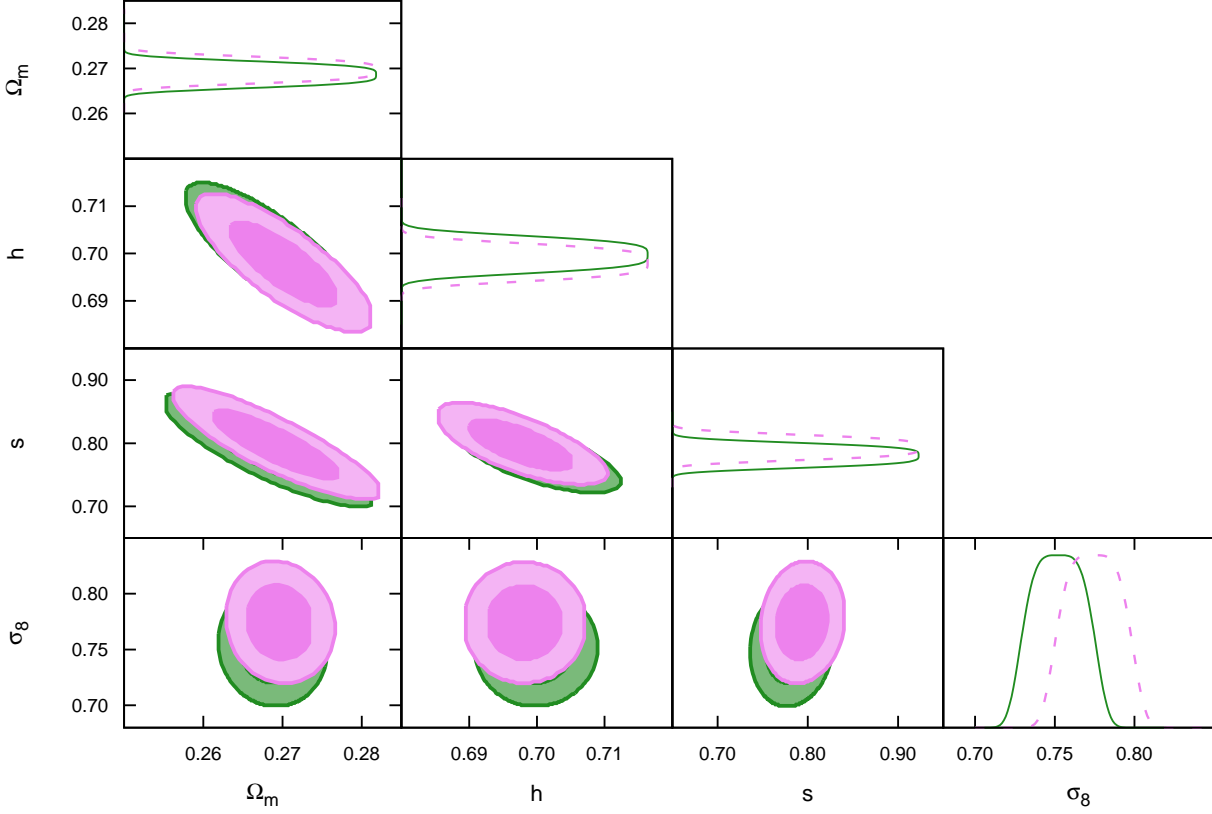


FIG. 5.  $1\sigma$  and  $2\sigma$  confidence regions for FCHDE and NCHDE models. Green background (violet foreground) area is for FCHDE (NCHDE) model. The likelihood function for FCHDE (NCHDE) has been shown by solid (dashed) curve.

Parameters	NCHDE	FCHDE
$\Omega_{m0}$	$0.269^{+0.0025+0.0034}_{-0.0023-0.0038}$	$0.268^{+0.0024+0.0031}_{-0.0021-0.0036}$
$h$	$0.693^{+0.004+0.006}_{-0.003-0.005}$	$0.695^{+0.003+0.006}_{-0.003-0.005}$
$s$	$0.792^{+0.027+0.064}_{-0.025-0.068}$	$0.780^{+0.026+0.069}_{-0.028-0.066}$
$\sigma_8$	$0.776^{+0.041+0.079}_{-0.043-0.078}$	$0.752^{+0.040+0.075}_{-0.043-0.077}$
$w_{d0}$	-1.051	-1.063

TABLE II. The best fit values of parameters using the joint analysis of geometry measurements data + growth rate data for NCHDE and FCHDE models.

- for the  $\Lambda$ CDM model,  $\chi^2_{\min} = 588.9$ ,  $n_{\text{fit}} = 3$  and  $\text{AIC}_\Lambda = 594.9$ .

In the case of geometrical and growth rate data,

- for the NCHDE model,  $\chi^2_{\min} = 595.8$ ,  $n_{\text{fit}} = 5$  and  $\text{AIC} = 605.8$ ;

- For FCHDE model,  $\chi^2_{\min} = 595.2$ ,  $n_{\text{fit}} = 5$  and  $\text{AIC} = 605.2$ ;
- for the  $\Lambda$ CDM model,  $\chi^2_{\min} = 595.9$ ,  $n_{\text{fit}} = 4$  and  $\text{AIC}_\Lambda = 603.9$

The above results show that in all possible cases  $\Delta\text{AIC} = |\text{AIC} - \text{AIC}_\Lambda| \leq 2$  which implies that the observational data are consistent with the current cosmological models (for a relevant discussion see Ref.[40]). Also in figure (5) we present the  $1\sigma$  and  $2\sigma$  combined likelihood contours for the explored holographic DE models (FCHDE: green region and NCHDE: violet region). We observe that both HDE models (FCHDE and NCHDE) provide the same statistical results within  $1\sigma$  uncertainties.

To this end, using the aforesaid cosmological parameters in figure (6) we compare the observed (open boxes) with the theoretical evolution of the growth rate  $f\sigma_8(z)$ . Notice, that  $f(z)$  is the rate of the growing mode (see next section),  $\sigma_8(z) = \sigma_8 D(z)$  and  $D(z)$  is the growth factor normalized to unity at the present time. As is expected from the AIC analysis the current DE models

TABLE III. The  $f\sigma_8(z)$  data points including their references and surveys.

$z$	$f\sigma_8(z)$	Reference
0.02	$0.360 \pm 0.040$	[81]
0.067	$0.423 \pm 0.055$	[82]
0.10	$0.37 \pm 0.13$	[83]
0.17	$0.510 \pm 0.060$	[84]
0.35	$0.440 \pm 0.050$	[85, 86]
0.77	$0.490 \pm 0.180$	[85, 87]
0.25	$0.351 \pm 0.058$	[88]
0.37	$0.460 \pm 0.038$	[88]
0.22	$0.420 \pm 0.070$	[89]
0.41	$0.450 \pm 0.040$	[89]
0.60	$0.430 \pm 0.040$	[89]
0.60	$0.433 \pm 0.067$	[90]
0.78	$0.380 \pm 0.040$	[89]
0.57	$0.427 \pm 0.066$	[91]
0.30	$0.407 \pm 0.055$	[90]
0.40	$0.419 \pm 0.041$	[90]
0.50	$0.427 \pm 0.043$	[90]
0.80	$0.47 \pm 0.08$	[92]

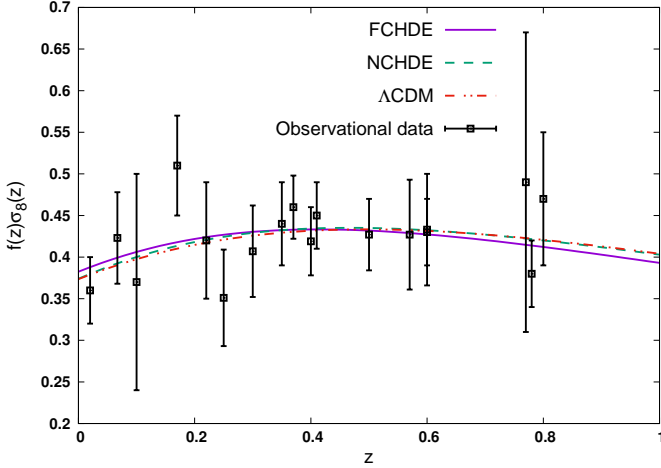


FIG. 6. The growth rate function of matter perturbations using the best fit values of cosmological parameters. The violet solid, green dashed and red dotted-double-dashed curves show the FCHDE, NCHDE and  $\Lambda$ CDM models, respectively. Observational data have been shown by open square with their error bars (see Table III).

provide almost the same growth rate predictions.

#### IV. THE GROWTH INDEX IN HOLOGRAPHIC COSMOLOGY

Let us focus now on the analysis of the growth index of matter perturbations  $\gamma$ . It is well known that the growth rate of clustering is given in terms  $\gamma$  and  $\Omega_m(a)$

(see Refs. [39, 93–99])

$$f(a) = \frac{d\ln\delta_m}{d\ln a} \simeq \Omega_m^\gamma(a). \quad (26)$$

Basically, for a given cosmological model the growth index of matter fluctuations provides a characteristic identity at the perturbation level. As an example, within the context of GR it has been shown that the asymptotic value of the growth index is  $\gamma_\infty = \frac{3(w-1)}{6w-5}$ , where in this case the dark energy EoS parameter is constant [93, 94, 96–98]. Of course, for the usual  $\Lambda$ CDM model ( $w = -1$ ) the above formula boils down to  $\gamma_\infty^{(\Lambda)} = 6/11$ . Notice, that for some specific types of modified gravity models we refer the reader to [96, 97, 100–105].

Now following the methodology of Abramo et al. [42, 43] we write the following equation

$$\ddot{\delta}_m + 2H\dot{\delta}_m = \frac{3H^2}{2} [\Omega_m\delta_m + \Omega_d\delta_d(1 + 3c_{\text{eff}}^2)]. \quad (27)$$

Changing the variables from  $t$  to  $a$  ( $\frac{d\delta_m}{dt} = aH\frac{d\delta_m}{da}$ ) we obtain

$$a^2\delta_m'' + a\left(3 + \frac{\dot{H}}{H^2}\right)\delta_m' = \frac{3}{2} [\Omega_m\delta_m + (1 + 3c_{\text{eff}}^2)\Omega_d\delta_d], \quad (28)$$

where

$$\frac{\dot{H}}{H^2} = \frac{d\ln H}{d\ln a} = -\frac{3}{2} - \frac{3}{2}w_d(a)\Omega_d(a), \quad (29)$$

and  $\Omega_d(a) = 1 - \Omega_m(a)$ . Of course, for  $c_{\text{eff}}^2 = 0$  (FCHDE model) Eq.(28) reduces to Eq.(18) as it should. We would like to point that by definition in the case of the  $\Lambda$ CDM model DE perturbations vanish,  $\delta_d \equiv 0$ .

Furthermore, based on the above and utilizing the first equality of Eq.(26) it is easy to prove that

$$\frac{df}{d\ln a} + \left(2 + \frac{d\ln H}{d\ln a}\right)f + f^2 = \frac{3\mu\Omega_m}{2}, \quad (30)$$

or

$$-(1+z)\frac{d\gamma}{dz}\ln(\Omega_m) + \Omega_m^\gamma + 3w_d\Omega_d\left(\gamma - \frac{1}{2}\right) + \frac{1}{2} = \frac{3}{2}\Omega_m^{1-\gamma}\mu. \quad (31)$$

where we have inserted  $f(z) = \Omega_m(z)^{\gamma(z)}$ , Eq.(29) and  $\frac{df}{da} = -(1+z)^{-2}\frac{df}{dz}$  in Eq.(30). Also, the quantity  $\mu(a)$ , which characterizes the status of the HDE, is given by

$$\mu(a) = \begin{cases} 1 & \text{Homogeneous HDE} \\ 1 + \frac{\Omega_d(a)}{\Omega_m(a)}\Delta_d(a)(1 + 3c_{\text{eff}}^2) & \text{Clustered HDE} \end{cases} \quad (32)$$

where  $\Delta_d \equiv \delta_d/\delta_m$ . Notice, that below we use the abbreviation CHDE which corresponds to clustered holographic dark energy model with  $c_{\text{eff}}^2 \neq 0$ . Of course, for  $c_{\text{eff}}^2 = 0$  we recover the fully clustered case (FCHDE model see section II).

It has been proposed that an approximated solution of Eq.(31) is written as a first order Taylor expansion around the present epoch  $a(z) = 1$  (see Refs. [106],[107],[108],[109–112])

$$\gamma(a) = \gamma_0 + \gamma_1 [1 - a(z)] . \quad (33)$$

where  $a(z) = 1/(1+z)$ . Furthermore, evaluating Eq.(31) for  $z = 0$  and with the aid of Eq.(33) we can write the coefficient  $\gamma_1$  as a function of  $(\Omega_{m0}, \gamma_0, w_{d0}, \mu_0)$  (see also Ref.[113])

$$\gamma_1 = \frac{\Omega_{m0}^{\gamma_0} + 3w_{d0}(\gamma_0 - \frac{1}{2})\Omega_{d0} + \frac{1}{2} - \frac{3}{2}\Omega_{m0}^{1-\gamma_0}\mu_0}{\ln\Omega_{m0}} , \quad (34)$$

where  $\mu_0 = \mu(z=0)$  and  $w_{d0} = w_d(z=0)$ .

In order to obtain the evolution of the growth index (33) we need to know the value of  $\gamma_0$ . It is easy to check from Eq.(33) that  $\gamma_\infty \simeq \gamma_0 + \gamma_1$  at large redshift  $z \gg 1$  and thus  $\gamma_0 \simeq \gamma_\infty - \gamma_1$ . Therefore, it is important to calculate the asymptotic value of the growth index from first principles.

Fortunately, Steigward et al. [61] developed a general mathematical approach which provides  $\gamma_\infty$  analytically [see Eq.(8) in [61] and the discussion in [114]] for a large family of DE models. In particular, based on Steigward et al. [61] one can use

$$\gamma_\infty = \frac{3(M_0 + M_1) - 2(H_1 + N_1)}{2 + 2X_1 + 3M_0} \quad (35)$$

where the following quantities have been defined:

$$M_0 = \mu|_{\omega=0} , \quad M_1 = \left. \frac{d\mu}{d\omega} \right|_{\omega=0} \quad (36)$$

and

$$N_1 = 0 , \quad H_1 = -\frac{X_1}{2} = \frac{3}{2} w_d(a)|_{\omega=0} . \quad (37)$$

Notice, that in the notation of Steigward et al. [61] the basic cosmological functions are provided in terms of the variable  $\omega = \ln\Omega_m(a)$ . The latter implies that for  $z \gg 1$  we have  $\Omega_m(a) \rightarrow 1$  [or  $\Omega_d(a) \rightarrow 0$ ] and thus  $\omega \rightarrow 0$ .

Bellow we provide the main results of the above analysis.

#### A. Homogeneous HDE: NCHDE model

Considering the non-clustering holographic dark energy (NCHDE) model,  $\mu(a) = 1$ , we find [see Eqs.(36), (37)]

$$\{M_0, M_1, H_1, X_1\} = \{1, 0, \frac{3w_\infty}{2}, -3w_\infty\}$$

where we have used  $w_\infty \equiv w_d(a)_{\omega=0}$ . If we substitute the above coefficients into Eq.(35) then the asymptotic growth index is given by

$$\gamma_\infty = \frac{3(w_\infty - 1)}{6w_\infty - 5} . \quad (38)$$

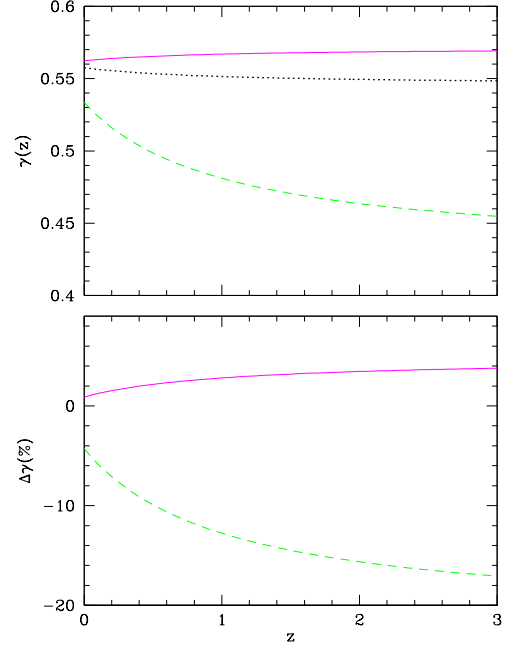


FIG. 7. *Upper Panel:* The growth index of matter perturbations (33) as a function of  $z$ . The lines are as follows. The results for NCHDE (solid curve) and FCHDE models are given by the solid and dashed curves. Also, the thin dotted line corresponds to the concordance  $\Lambda$  cosmology. *Bottom Panel:* The relative difference  $[1 - \gamma(z)/\gamma^{(\Lambda)}(z)]\%$  of the growth index for the NCHDE and FCHDE models with respect to  $\Lambda$ CDM.

As expected, we recover the standard  $\Lambda$ CDM value  $\gamma_\infty^{(\Lambda)} = 6/11$  for  $w_\infty = -1$ . In the case of holographic cosmology, namely  $w_\infty = -1/3$  we find  $\gamma_\infty^{(\text{NCHDE})} = 4/7$  which is somewhat larger ( $\sim 4.8\%$ ) than that of the concordance  $\Lambda$  cosmology.

Knowing the value of  $\gamma_\infty$ , inserting the expression  $\gamma_0 \simeq \gamma_\infty - \gamma_1$  into Eq.(34) and using the best fit values of the cosmological parameters (see Table II) we find  $(\gamma_0, \gamma_1)^{(\text{NCHDE})} \simeq (0.562, 0.09)$ . In the case of the  $\Lambda$ CDM we obtain  $(\gamma_0, \gamma_1) \simeq (0.557, -0.012)$ . In the upper panel of figure 5 we plot the growth index evolution (33) for the NCHDE (solid curve) and  $\Lambda$ CDM models (thin dotted curve) respectively. We observe that the growth index evolution of the NCHDE model is somewhat larger than the  $\Lambda$ CDM cosmological model. Specifically, we find that the corresponding relative deviations (see bottom panel of Fig.5) are  $[1 - \gamma^{(\text{NCHDE})}/\gamma^{(\Lambda)}] \sim 3\%$ .

#### B. Clustered HDE: CHDE model

Now we concentrate on the clustered holographic DE in which the quantity  $\mu(a)$  is given by the second branch of Eq.(32). First of all we need to define the functional



form of  $\Delta_d$ . Based on Eqs.(7) and (22) we can write

$$\Delta_d = \frac{1 + w_d}{1 - 3w_d} = \frac{s - \sqrt{\Omega_d}}{3s + 3\sqrt{\Omega_d}} = \frac{s - \sqrt{1 - e^\omega}}{3s + 3\sqrt{1 - e^\omega}} \quad (39)$$

where  $e^\omega = \Omega_m(a) = 1 - \Omega_d(a)$ . Under the latter conditions  $\mu(\omega)$  is written as

$$\mu(\omega) = 1 + (1 + 3c_{\text{eff}}^2) \left( \frac{1 - e^\omega}{e^\omega} \right) \left( \frac{s - \sqrt{1 - e^\omega}}{3s + 3\sqrt{1 - e^\omega}} \right). \quad (40)$$

Therefore, from Eqs.(36) and (37) it is easy to show that

$$\{M_0, M_1, H_1, X_1\} = \{1, -\frac{(1 + 3c_{\text{eff}}^2)}{3}, \frac{3w_\infty}{2}, -3w_\infty\}$$

and for  $w_\infty = -1/3$  we get via Eq.(35)

$$\gamma_\infty^{(\text{CHDE})} = \frac{3(1 - c_{\text{eff}}^2)}{7}. \quad (41)$$

Obviously, if we set  $c_{\text{eff}}^2 = 0$  in the above equation then we provide the asymptotic value of the fully clustered HDE (FCHDE) model,  $\gamma_\infty^{(\text{FCHDE})} = 3/7$ . Finally, concerning the evolution of the growth index the situation is as follows. Substituting  $\gamma_0 \simeq \gamma_\infty^{(\text{FCHDE})} - \gamma_1$  into Eq.(34) and utilizing the cosmological parameters of Table II we get  $(\gamma_0, \gamma_1)^{(\text{FCHDE})} \simeq (0.534, -0.105)$ . The dashed curve in the upper panel of figure 5 corresponds to the evolution of  $\gamma(z)$  for the FCHDE model (dashed curve). In this case we verify that the growth index strongly deviates with respect to that of the usual  $\Lambda$  cosmology. For example close to the present epoch the departure can be of the order of  $[1 - \gamma^{(\text{FCHDE})}/\gamma^{(\Lambda)}] \sim -4\%$  while at relative large redshifts  $z \sim 1$  we get  $[1 - \gamma^{(\text{FCHDE})}/\gamma^{(\Lambda)}] \sim -13\%$ .

## V. CONCLUSION

In this work we investigated the performance of the holographic dark energy (HDE) model which is originated from the holographic principle in quantum gravity theory [14]. First we studied the growth of matter perturbations in clustered HDE models and discussed the differences from the homogeneous case. Second we performed a joint likelihood analysis using the latest observational

data in order to place tight constraints on the cosmological parameters. Lastly, we provided (for the first time) the growth index of matter perturbations for the homogeneous and inhomogeneous HDE models. Specifically, the main results of the current work are summarized as follows:

(i) We find that for  $s < 0.6$  the amplitude of matter perturbations  $\delta_m$  of both clustered and homogeneous HDE models are larger than those of the concordance  $\Lambda$  cosmology, while the opposite holds for  $s > 0.6$ . Notice, that  $s$  is a constant which is related with the holographic DE density [see Eq. 1]. Moreover, the relative deviation between clustered and homogeneous HDE cosmologies remains small in the case of phantom HDE, while there are differences in the case of quintessence HDE models (see Fig. 2). As far as the growth rate of clustering,  $f(a)$ , is concerned we find that for the clustered HDE models  $f(a)$  is always larger than that of the concordance  $\Lambda$ CDM model. In the case of homogeneous HDE models the growth rate of clustering depends on the value of  $s$ , namely  $f(a) > f_\Lambda(a)$  for  $s < 0.7$  (the opposite holds for  $s > 0.7$ : see Fig. 3).

(ii) The overall likelihood analysis showed that both clustered and homogeneous HDE models provide the same cosmological parameters within  $1\sigma$  uncertainties. In this context based on the AIC analysis we found that the HDE models are consistent with the observational data.

(iii) Finally, we focused our analysis on the growth index of matter fluctuations. Assuming that the holographic dark energy is homogeneous then the asymptotic value of the growth index of matter perturbations is given by  $\gamma \approx 4/7$  which differs by  $\sim 4.8\%$  from that of  $\Lambda$ CDM,  $\gamma^{(\Lambda)} \approx 6/11$ . The situation is different in the case of inhomogeneous holographic dark energy. Within this framework, we investigated the growth index and we verified that it is strongly affected by the dark energy perturbations. In particular, we found  $\gamma \approx 3(1 - c_{\text{eff}}^2)/7$ , where  $c_{\text{eff}}^2$  is the effective sound speed. Finally, assuming that the dark energy is allowed to cluster in a similar fashion to dark matter ( $c_{\text{eff}}^2 = 0$ ) we find that the asymptotic value of the growth index ( $\gamma \approx 3/7$ ) is strongly affected by the DE perturbations. Such an effect can be used, especially in the light of the next generation of surveys [115], in order to test whether the DE perturbations appear in the observed universe. In other words, if one is able to show that the observed growth index is close to  $\sim 3/7$  then this is a hint that holographic DE perturbations exist in nature.

---

[1] A. G. Riess *et al.* (Supernova Search Team), *Astron. J.* **116**, 1009 (1998), arXiv:astro-ph/9805201 [astro-ph].  
 [2] S. Perlmutter *et al.* (Supernova Cosmology Project), *Astrophys. J.* **517**, 565 (1999), arXiv:astro-ph/9812133 [astro-ph].

[3] M. Kowalski *et al.* (Supernova Cosmology Project), *Astrophys. J.* **686**, 749 (2008), arXiv:0804.4142 [astro-ph].  
 [4] G. Hinshaw *et al.* (WMAP), *Astrophys. J. Suppl.* **180**, 225 (2009), arXiv:0803.0732 [astro-ph].

- [5] P. A. R. Ade *et al.* (Planck), *Astron. Astrophys.* **571**, A16 (2014), arXiv:1303.5076 [astro-ph.CO].
- [6] E. J. Copeland, M. Sami, and S. Tsujikawa, *Int. J. Mod. Phys. D* **15**, 1753 (2006), arXiv:hep-th/0603057 [hep-th].
- [7] V. Sahni and A. A. Starobinsky, *Int. J. Mod. Phys. D* **9**, 373 (2000), arXiv:astro-ph/9904398 [astro-ph].
- [8] S. Weinberg, *Rev. Mod. Phys.* **61**, 1 (1989).
- [9] S. M. Carroll, *Living Rev. Rel.* **4**, 1 (2001), arXiv:astro-ph/0004075 [astro-ph].
- [10] P. J. E. Peebles and B. Ratra, *Rev. Mod. Phys.* **75**, 559 (2003), arXiv:astro-ph/0207347 [astro-ph].
- [11] T. Padmanabhan, *Phys. Rept.* **380**, 235 (2003), arXiv:hep-th/0212290 [hep-th].
- [12] M. Li, X.-D. Li, S. Wang, and Y. Wang, *Commun. Theor. Phys.* **56**, 525 (2011), arXiv:1103.5870 [astro-ph.CO].
- [13] K. Bamba, S. Capozziello, S. Nojiri, and S. D. Odintsov, *Astrophys. Space Sci.* **342**, 155 (2012), arXiv:1205.3421 [gr-qc].
- [14] L. Susskind, *J. Math. Phys.* **36**, 6377 (1995), arXiv:hep-th/9409089 [hep-th].
- [15] A. G. Cohen, D. B. Kaplan, and A. E. Nelson, *Phys. Rev. Lett.* **82**, 4971 (1999), arXiv:hep-th/9803132 [hep-th].
- [16] Y. J. Ng, *Phys. Rev. Lett.* **86**, 2946 (2001), [Erratum: *Phys. Rev. Lett.* **88**, 139902 (2002)], arXiv:gr-qc/0006105 [gr-qc].
- [17] M. Arzano, T. W. Kephart, and Y. J. Ng, *Phys. Lett. B* **649**, 243 (2007), arXiv:gr-qc/0605117 [gr-qc].
- [18] P. Horava and D. Minic, *Phys. Rev. Lett.* **85**, 1610 (2000), arXiv:hep-th/0001145 [hep-th].
- [19] M. Cataldo, N. Cruz, S. del Campo, and S. Lepe, *Phys. Lett. B* **509**, 138 (2001), arXiv:gr-qc/0104028 [gr-qc].
- [20] S. D. Thomas, *Phys. Rev. Lett.* **89**, 081301 (2002).
- [21] S. D. H. Hsu, *Phys. Lett. B* **594**, 13 (2004), arXiv:hep-th/0403052 [hep-th].
- [22] M. Li, *Phys. Lett. B* **603**, 1 (2004), arXiv:hep-th/0403127 [hep-th].
- [23] D. Pavon and W. Zimdahl, *Phys. Lett. B* **628**, 206 (2005), arXiv:gr-qc/0505020 [gr-qc].
- [24] W. Zimdahl and D. Pavon, *Class. Quant. Grav.* **24**, 5461 (2007).
- [25] A. Sheykhi, *Phys. Rev. D* **84**, 107302 (2011), arXiv:1106.5697 [physics.gen-ph].
- [26] Q.-G. Huang and Y.-G. Gong, *JCAP* **0408**, 006 (2004), arXiv:astro-ph/0403590 [astro-ph].
- [27] H.-C. Kao, W.-L. Lee, and F.-L. Lin, *Phys. Rev. D* **71**, 123518 (2005), arXiv:astro-ph/0501487 [astro-ph].
- [28] X. Zhang and F.-Q. Wu, *Phys. Rev. D* **72**, 043524 (2005), arXiv:astro-ph/0506310 [astro-ph].
- [29] B. Wang, C.-Y. Lin, and E. Abdalla, *Phys. Lett. B* **637**, 357 (2006), arXiv:hep-th/0509107 [hep-th].
- [30] Z. Chang, F.-Q. Wu, and X. Zhang, *Phys. Lett. B* **633**, 14 (2006), arXiv:astro-ph/0509531 [astro-ph].
- [31] X. Zhang and F.-Q. Wu, *Phys. Rev. D* **76**, 023502 (2007), arXiv:astro-ph/0701405 [astro-ph].
- [32] S. M. R. Micheletti, *JCAP* **1005**, 009 (2010), arXiv:0912.3992 [gr-qc].
- [33] L. Xu, *Phys. Rev. D* **85**, 123505 (2012), arXiv:1205.2130 [astro-ph.CO].
- [34] M.-J. Zhang, C. Ma, Z.-S. Zhang, Z.-X. Zhai, and T.-J. Zhang, *Phys. Rev. D* **88**, 063534 (2013), arXiv:1303.0384 [astro-ph.CO].
- [35] M. Li, X.-D. Li, Y.-Z. Ma, X. Zhang, and Z. Zhang, *JCAP* **1309**, 021 (2013), arXiv:1305.5302 [astro-ph.CO].
- [36] J.-F. Zhang, M.-M. Zhao, J.-L. Cui, and X. Zhang, *Eur. Phys. J. C* **74**, 3178 (2014), arXiv:1409.6078 [astro-ph.CO].
- [37] J.-F. Zhang, M.-M. Zhao, Y.-H. Li, and X. Zhang, *JCAP* **1504**, 038 (2015), arXiv:1502.04028 [astro-ph.CO].
- [38] M. Tegmark *et al.* (SDSS), *Phys. Rev. D* **69**, 103501 (2004), arXiv:astro-ph/0310723 [astro-ph].
- [39] P. J. E. Peebles, *Principles of physical cosmology* (Princeton University Press, 1993).
- [40] A. Mehrabi, S. Basilakos, and F. Pace, *MNRAS* **452**, 2930 (2015), arXiv:1504.01262 [astro-ph.CO].
- [41] L. Xu, *Phys. Rev. D* **87**, 043525 (2013), arXiv:1302.2291 [astro-ph.CO].
- [42] L. R. Abramo, R. C. Batista, L. Liberato, and R. Rosenfeld, *JCAP* **0711**, 012 (2007), arXiv:0707.2882 [astro-ph].
- [43] L. R. Abramo, R. C. Batista, L. Liberato, and R. Rosenfeld, *Phys. Rev. D* **79**, 023516 (2009), arXiv:0806.3461 [astro-ph].
- [44] R. C. Batista and F. Pace, *JCAP* **1306**, 044 (2013), arXiv:1303.0414 [astro-ph.CO].
- [45] A. Mehrabi, M. Malekjani, and F. Pace, *Astrophys. Space Sci.* **356**, 129 (2015).
- [46] M. Li, C. Lin, and Y. Wang, *JCAP* **0805**, 023 (2008), arXiv:0801.1407 [astro-ph].
- [47] C. Armendariz-Picon, T. Damour, and V. F. Mukhanov, *Phys. Lett. B* **458**, 209 (1999).
- [48] C. Armendariz-Picon, V. F. Mukhanov, and P. J. Steinhardt, *Phys. Rev. D* **63**, 103510 (2001), arXiv:astro-ph/0006373 [astro-ph].
- [49] J. Garriga and V. F. Mukhanov, *Phys. Lett. B* **458**, 219 (1999), arXiv:hep-th/9904176 [hep-th].
- [50] R. Akhoury, D. Garfinkle, and R. Saotome, *JHEP* **1104**, 096 (2011).
- [51] J. K. Erickson, R. Caldwell, P. J. Steinhardt, C. Armendariz-Picon, and V. F. Mukhanov, *Phys. Rev. Lett.* **88**, 121301 (2002).
- [52] R. Bean and O. Doré, *Phys. Rev. D* **69**, 083503 (2004).
- [53] W. Hu and R. Scranton, *Phys. Rev. D* **70**, 123002 (2004).
- [54] G. Ballesteros and A. Riotto, *Phys. Lett. B* **668**, 171 (2008).
- [55] R. de Putter, D. Huterer, and E. V. Linder, *Phys. Rev. D* **81**, 103513 (2010).
- [56] D. Sapone and E. Majerotto, *Phys. Rev. D* **85**, 123529 (2012).

- [57] J. Dossett and M. Ishak, Phys. Rev. D **D88**, 103008 (2013).
- [58] T. Basse, O. E. Bjaelde, J. Hamann, S. Hannestad, and Y. Y. Wong, JCAP **1405**, 021 (2014).
- [59] R. C. Batista, Phys. Rev. D **89**, 123508 (2014).
- [60] F. Pace, R. C. Batista, and A. Del Popolo, MNRAS **445**, 648 (2014).
- [61] H. Steigerwald, J. Bel, and C. Marinoni, JCAP **1405**, 042 (2014).
- [62] S. Basilakos, J. Bueno Sanchez, and L. Perivolaropoulos, Phys. Rev. D **80**, 043530 (2009).
- [63] S. Basilakos, Mon. Not. Roy. Astron. Soc. **449**, 2151 (2015), arXiv:1412.2234 [astro-ph.CO].
- [64] S. Nesseris and D. Sapone, Int. J. Mod. Phys. **D24**, 1550045 (2015), arXiv:1409.3697 [astro-ph.CO].
- [65] Y. S. Myung, Phys. Lett. **B652**, 223 (2007), arXiv:0706.3757 [gr-qc].
- [66] When we deal with the growth of matter DE fluctuations we neglect the radiation component because we are well inside the matter era.
- [67] For an imperfect DE fluid see [52].
- [68] N. Suzuki, D. Rubin, C. Lidman, G. Aldering, and et.al, ApJ **746**, 85 (2012).
- [69] F. Beutler, C. Blake, M. Colless, D. H. Jones, L. Staveley-Smith, et al., MNRAS **416**, 3017 (2011).
- [70] N. Padmanabhan, X. Xu, D. J. Eisenstein, R. Scalzo, A. J. Cuesta, et al., MNRAS **427**, 2132 (2012).
- [71] L. Anderson, E. Aubourg, S. Bailey, D. Bizyaev, M. Blanton, et al., MNRAS **427**, 3435 (2013).
- [72] C. Blake, E. Kazin, F. Beutler, T. Davis, D. Parkinson, et al., MNRAS **418**, 1707 (2011).
- [73] G. Hinshaw et al. (WMAP), ApJS **208**, 19 (2013).
- [74] P. Serra, A. Cooray, D. E. Holz, A. Melchiorri, S. Pandolfi, and D. Sarkar, Phys. Rev. **D80**, 121302 (2009), arXiv:0908.3186 [astro-ph.CO].
- [75] S. Burles, K. M. Nollett, and M. S. Turner, Astrophys. J. **552**, L1 (2001), arXiv:astro-ph/0010171 [astro-ph].
- [76] M. Moresco et al., JCAP **1208**, 006 (2012), arXiv:1201.3609 [astro-ph.CO].
- [77] E. Gaztanaga, A. Cabre, and L. Hui, Mon. Not. Roy. Astron. Soc. **399**, 1663 (2009), arXiv:0807.3551 [astro-ph].
- [78] C. Blake et al., Mon. Not. Roy. Astron. Soc. **425**, 405 (2012), arXiv:1204.3674 [astro-ph.CO].
- [79] L. Anderson et al. (BOSS), Mon. Not. Roy. Astron. Soc. **441**, 24 (2014), arXiv:1312.4877 [astro-ph.CO].
- [80]  $N/n_{\text{fit}} > 0$ , the Akaike information criterion is given by  $\text{AIC} = \chi^2_{\text{min}} + 2n_{\text{fit}}$ , where  $n_{\text{fit}}$  is the number of free parameter [116].
- [81] M. J. Hudson and S. J. Turnbull, Astrophys. J. **751**, L30 (2013), arXiv:1203.4814 [astro-ph.CO].
- [82] F. Beutler, C. Blake, M. Colless, D. H. Jones, L. Staveley-Smith, G. B. Poole, L. Campbell, Q. Parker, W. Saunders, and F. Watson, Mon. Not. Roy. Astron. Soc. **423**, 3430 (2012), arXiv:1204.4725 [astro-ph.CO].
- [83] M. Feix, A. Nusser, and E. Branchini, ArXiv e-prints, 1503.05945 (2015).
- [84] W. J. Percival et al. (2dFGRS), Mon. Not. Roy. Astron. Soc. **353**, 1201 (2004), arXiv:astro-ph/0406513 [astro-ph].
- [85] Y.-S. Song and W. J. Percival, JCAP **0910**, 004 (2009), arXiv:0807.0810 [astro-ph].
- [86] M. Tegmark et al. (SDSS Collaboration), Phys. Rev. D **74**, 123507 (2006).
- [87] L. Guzzo et al., Nature **451**, 541 (2008), arXiv:0802.1944 [astro-ph].
- [88] L. Samushia, W. J. Percival, and A. Racca- nelli, Mon. Not. Roy. Astron. Soc. **420**, 2102 (2012), arXiv:1102.1014 [astro-ph.CO].
- [89] C. Blake et al., Mon. Not. Roy. Astron. Soc. **415**, 2876 (2011), arXiv:1104.2948 [astro-ph.CO].
- [90] R. Tojeiro, W. Percival, J. Brinkmann, J. Brownstein, D. Eisenstein, et al., MNRAS **424**, 2339 (2012).
- [91] B. A. Reid, L. Samushia, M. White, W. J. Percival, M. Manera, et al., MNRAS **426**, 2719 (2012).
- [92] S. de la Torre, L. Guzzo, J. Peacock, E. Branchini, A. Iovino, et al., A&A **557**, A54 (2013).
- [93] V. Silveira and I. Waga, Phys. Rev. **D50**, 4890 (1994).
- [94] L.-M. Wang and P. J. Steinhardt, Astrophys. J. **508**, 483 (1998), arXiv:astro-ph/9804015 [astro-ph].
- [95] E. V. Linder and A. Jenkins, Mon. Not. Roy. Astron. Soc. **346**, 573 (2003), arXiv:astro-ph/0305286 [astro-ph].
- [96] E. V. Linder, Phys. Rev. **D70**, 023511 (2004), arXiv:astro-ph/0402503 [astro-ph].
- [97] E. V. Linder and R. N. Cahn, Astropart. Phys. **28**, 481 (2007), arXiv:astro-ph/0701317 [astro-ph].
- [98] S. Nesseris and L. Perivolaropoulos, Phys. Rev. **D77**, 023504 (2008), arXiv:0710.1092 [astro-ph].
- [99] A. Lue, R. Scoccimarro, and G. D. Starkman, Phys. Rev. **D69**, 124015 (2004), arXiv:astro-ph/0401515 [astro-ph].
- [100] H. Wei, Phys. Lett. **B664**, 1 (2008), arXiv:0802.4122 [astro-ph].
- [101] Y. Gong, Phys. Rev. **D78**, 123010 (2008), arXiv:0808.1316 [astro-ph].
- [102] X.-y. Fu, P.-x. Wu, and H.-w. Yu, Phys. Lett. **B677**, 12 (2009), arXiv:0905.1735 [gr-qc].
- [103] R. Gannouji, B. Moraes, and D. Polarski, JCAP **0902**, 034 (2009), arXiv:0809.3374 [astro-ph].
- [104] S. Tsujikawa, R. Gannouji, B. Moraes, and D. Polarski, Phys. Rev. **D80**, 084044 (2009), arXiv:0908.2669 [astro-ph.CO].
- [105] S. Basilakos and P. Stavrin- nos, Phys. Rev. **D87**, 043506 (2013), arXiv:1301.4327 [gr-qc].
- [106] M. Ishak and J. Dossett, Phys. Rev. **D80**, 043004 (2009), arXiv:0905.2470 [astro-ph.CO].
- [107] A. B. Belloso, J. Garcia-Bellido, and D. Sapone, JCAP **1110**, 010 (2011), arXiv:1105.4825 [astro-ph.CO].
- [108] C. Di Porto, L. Amendola, and E. Branchini, Mon. Not. Roy. Astron. Soc. **419**, 985 (2012), arXiv:1101.2453 [astro-ph.CO].
- [109] A. Pouri, S. Basilakos, and M. Plionis, JCAP **1408**, 042 (2014), arXiv:1402.0964 [astro-ph.CO].
- [110] S. Basilakos and A. Pouri, MNRAS **423**, 3761 (2012), arXiv:1203.6724 [astro-ph.CO].

- [111] S. Basilakos, Int. J. Mod. Phys. **D21**, 1250064 (2012), arXiv:1202.1637 [astro-ph.CO].
- [112] P. Wu, H. W. Yu, and X. Fu, JCAP **0906**, 019 (2009), arXiv:0905.3444 [gr-qc].
- [113] D. Polarski and R. Gannouji, Phys. Lett. **B660**, 439 (2008), arXiv:0710.1510 [astro-ph].
- [114] S. Basilakos and J. Sol, (2015), arXiv:1509.06732 [astro-ph.CO].
- [115] D. Sapone, E. Majerotto, M. Kunz, and B. Garilli, Phys. Rev. **D88**, 043503 (2013), arXiv:1305.1942 [astro-ph.CO].
- [116] H. Akaike, IEEE Transactions of Automatic Control **19**, 716 (1974).